

Estimation of Driver Reaction Time from Car-Following Data

Application in Evaluation of General Motor-Type Model

Xiaoliang Ma and Ingmar Andréasson

Driver behavior plays an important role in modeling vehicle dynamics in a traffic simulation environment. To study one element of general driver behavior, that of car following, an advanced-instrumented vehicle has been applied in dynamic data collection in real-traffic flow on Swedish roads. This paper briefly introduces the car-following data collection and smoothing methods. Moreover, spectrum analysis methods based on Fourier analysis of car-following data are introduced to estimate driver reaction times, a crucial parameter of driver behavior. A generalized general motor-type model was calibrated, an extension of the classic nonlinear general motor model, in a stable following regime based on estimated driver reaction times. The calibrated model was then evaluated by closed-loop simulations.

Driver behavior is an important factor for evaluating modern transportation systems. The new technologies in the form of intelligent transportation systems (ITS) make understanding the behavioral response of drivers more necessary than ever. In contrast, ITS technologies offer modern researchers a good opportunity to observe and analyze human behavior in different real-traffic situations. Recently, the use of microscopic simulation to assess the effects of new ITS systems both on-road and in-vehicle has become increasingly popular and credibility of the simulation models is crucial to their successful applications. Hence, calibration of the model based on measurements from a real-traffic environment attracts increased attention in transportation and traffic planning.

In microscopic traffic simulation, driver behavior is one of the most important parts of the models to reflect general traffic characteristics. Moreover, the car-following model is an essential component of driver behavior models. Therefore, calibration or adjustment of parameters of the car-following model directly affects the applicability of the simulation models.

CAR-FOLLOWING BEHAVIOR

Car-following models describe the longitudinal behavior of drivers when they are following a leading vehicle and trying to maintain a driver-specific safe headway distance to that vehicle. Normally, the driver in the car-following stage is assumed to move forward without the intention of changing lane or overtaking. Research of driving

behavior in traffic science can be traced back to the 1950s when traffic flow theory was initially developed and car-following models were extensively studied. The well-known mathematical car-following model introduced by Gazis et al. in 1961 (1) was both an extension of the early models [e.g., Chandler et al. (2)] and a summary of the early idea of stimulus-response-type car-following models. The model takes the form of a differential equation

$$a_n(t + \tau_n) = \alpha \frac{v_n(t + \tau_n)^\beta}{[x_{n-1}(t) - x_n(t)]^\gamma} [v_{n-1}(t) - v_n(t)] \quad (1)$$

where

$x(t)$, $v(t)$, and $a(t)$ = position, speed, and acceleration of the vehicles;

τ_n = reaction time of the driver, assumed to be a fixed value for a certain driver n ; and

α , β , and γ = constant parameters.

This model, often called the nonlinear general motor (GM) model, has the intuitive hypothesis that the follower's acceleration is proportional to the speed difference, $\delta v(t) = v_{n-1}(t) - v_n(t)$, and the exponent of its own speed but is inversely proportional to distance headway, $D(t) = x_{n-1}(t) - x_n(t)$. The speed difference part on the right-hand side is always translated as the "stimulus" term, whereas the fraction between the exponent of following speed and that of distance headway is called the sensitivity term. The nonlinear GM model has been calibrated on different data sets by many researchers, although a variety of estimated parameter sets were reported (3). Besides the GM-type models, there are many other model forms such as fuzzy inference models (4) and action point models (5). Recent research on this basic topic of traffic science has shown promising progress, which promotes both the elementary research of human behavior science and its applications in traffic engineering.

DRIVER REACTION DELAY

Reaction delay is a common characteristic of humans in operation and control, such as driving a car. The operational coefficients and delay characteristic of humans can vary rapidly due to changes in factors such as task demands, motivation, workload, and fatigue (6). However, estimation of these variations is almost impossible in the classic paradigms. Therefore, an assumption of a fixed reaction delay in a certain regime still cannot be completely circumvented. Driver reaction time was defined as the summation of perception time and foot movement time by earlier car-following research (7). In psychological

Center for Traffic Simulation Research, Royal Institute of Technology, Teknikringen 72, Stockholm 10044, Sweden.

Transportation Research Record: Journal of the Transportation Research Board, No. 1965, Transportation Research Board of the National Academies, Washington, D.C., 2006, pp. 130-141.

studies, the driver reaction process is further represented in four states: perception, recognition, decision, and physical response. In microscopic traffic simulation, the driver and vehicle are normally modeled as an integrated unit and the delay within the mechanical system of the vehicle is often neglected. Although research on car-following models historically has focused on exploration of different modeling frameworks and variables that affect this behavior, it has been recognized that the reaction delay τ_n of each driver n is an indispensable factor for the identification of car-following models. It affects the traffic dynamics not only in a microscopic way but also macroscopically (8). Many studies have estimated the reaction time based on indoor experiments and driving simulators. For example, in the study by Johansson and Rummel (9) more than 300 subjects were instructed to press a pedal as soon as they heard a sound. The estimated reaction time varied from 0.4 to 2.7 s, with a mean value of 1.0 s. A recent study using both a real driving environment and a simulator (10) indicates that the reaction time of drivers to an anticipated danger in a real environment has a mean value of 0.42 s and a standard deviation of 0.14 s, whereas the mean value of the reaction time distribution to an unanticipated danger by extreme braking is about 1.1 s, and that in a simulator is about 0.9 s. In real traffic, the driver reactions to expected and unexpected stimuli are also different; Fambro et al. (11) reported that the mean reaction times for unexpected and expected stimuli are 1.3 and 0.7 s, respectively. To estimate driver reaction delays from real data, several approaches have been proposed. Ozaki (12) developed a graphic method to identify the individual driver reaction time based on speed difference and acceleration profiles. Ranjitkar et al. (13) applied the graphic method in stability analysis of car-following behaviors and, on the basis of car-following data collected on a test track, they estimated that the average driver reaction time for individual drivers ranged from 1.27 to 1.55 s. Ahmed (14) computed the reaction time jointly with other parameters of the car-following model, and the estimated mean value of reaction times was 1.34 s. The reaction time distribution, assumed lognormal, was estimated from empirical data using the maximum-likelihood method under assumptions of a predetermined GM-type model form.

OBJECTIVE AND STRUCTURE

To study general driver behavior and identify parameters of car-following models for microsimulation, an advanced instrumented vehicle has been applied to collect data using a high measurement frequency in real traffic on Swedish roads. The collected data are smoothed with the Kalman smoothing algorithm and then analyzed in the frequency domain on the basis of Fourier transform and spectrum analysis, through which the reaction delay time can be estimated for each driver observed. On the basis of estimated delay and smoothed data, a car-following database was created for model calibration and evaluation purposes.

This article is organized as follows: the data collection method for this study is briefly introduced; then the mathematical foundation of spectrum analysis and its applications in the driver reaction delay estimation are illustrated; a generalized GM-type model is calibrated on the basis of reaction times identified by spectrum analysis methods and then the model is evaluated with data from the car-following database; finally, the paper is summarized and conclusions are drawn. Reaction delay is a common characteristic of humans in operation and control, such as driving a car. The operational coefficients and delay characteristic of humans can vary rapidly because of changes in factors such as task demands.

DATA COLLECTION AND CAR-FOLLOWING REGIMES

An instrumented vehicle developed by Volvo Technology was used in the car-following data collection. The car was equipped with a navigation system based on a Global Positioning System and an onboard trip computer for recording travel time, distance, speed, and fuel economy. Two lidar sensors and corresponding video cameras were installed to observe objects in the front and rear directions. Each lidar sensor can capture at most four objects at the same time. The distance between the instrumented car and the observed object can be measured continuously by sensors at a maximal frequency of 50 times per second (Hz)—that is, the measuring interval is $\Delta t = 0.02$ s. Meanwhile, the Volvo ERS software installed on a portable computer connected to the equipment assembled all infused information, synchronized it with video signals, and then wrote it as a binary file. A real-time adaptive filtering algorithm was adopted in the software to smooth the measured distance data, from which relative speed and acceleration were numerically approximated. Hence, the data and traffic situations can be compared and analyzed at the same time using the software. Figure 1a shows the interface of the Volvo ERS logger. The car-following data collected can be written as follows:

$$x(t) = [s_i(t) \ v_i(t) \ a_i(t) \ D(t) \ dv(t) \ da(t)]^T$$

where

$s_i(t)$, $v_i(t)$, and $a_i(t)$ = position, speed, and acceleration of instrumented vehicle i and

$D(t)$, $dv(t)$, and $da(t)$ = relative position, speed, and acceleration between instrumented car and observed car.

The car-following experiments were at this time mostly conducted on a motorway section of Road E18 near Stockholm, with speed limits of 70 and 90 km/h. A follow-the-leader behavior of random vehicles behind the equipped car was observed. The motorway section includes the “2+1” type road where “pure” car-following behavior can be mostly captured in the single-lane parts. The unique features of the equipped car and the high measuring frequency provide an opportunity to obtain car-following data of high quality from real traffic. However, relative speed and acceleration profiles are derived based on real-time adaptive filtering of the distance measurement, by which certain delays might be introduced and the filtering results are not smooth enough for the car-following study. In an earlier publication (15), a state-space model was formulated for the tracked vehicles based on existing physical relations in vehicle states and on a random walk model of acceleration time series. The model can be represented as follows:

$$X(t+1) = F \cdot X(t) + V(t) \quad (2)$$

$$Y(t) = H \cdot X(t) + W(t) \quad (3)$$

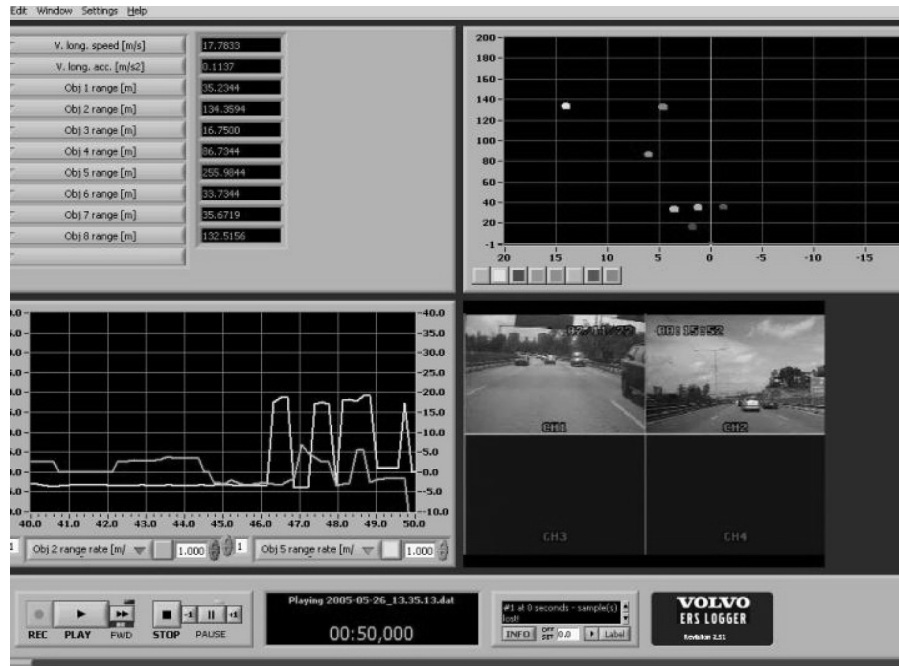
where

$X(t) = [s_n(t) \ v_n(t) \ a_n(t)]^T$ = physical state vector of position, speed, and acceleration;

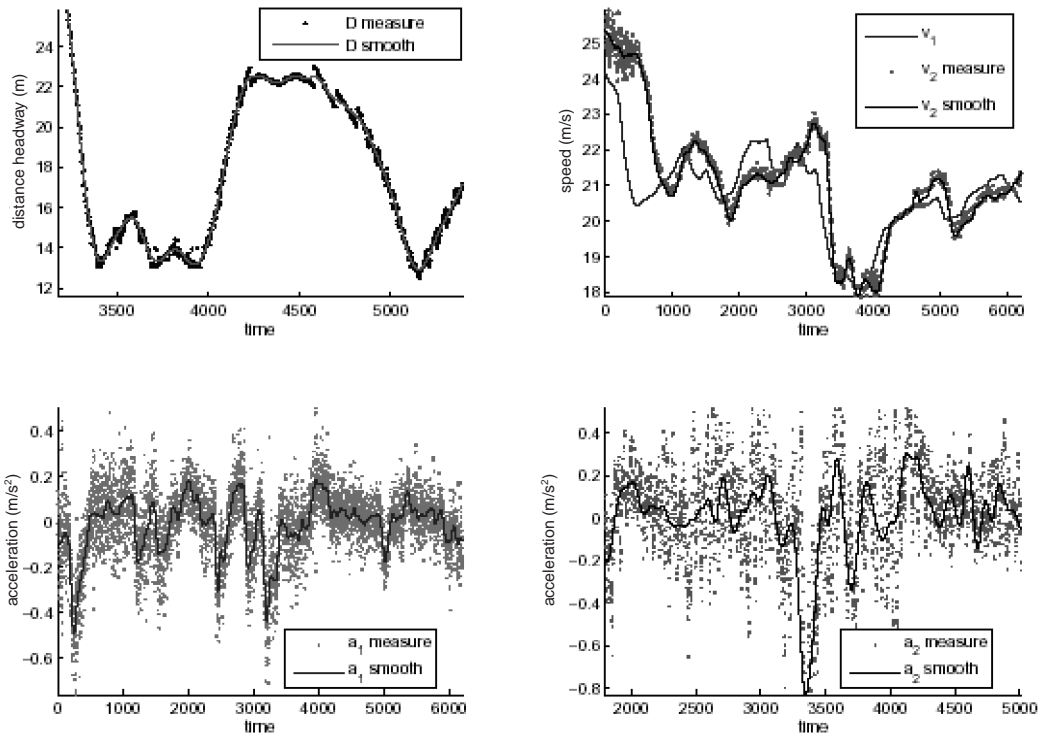
$V(t) = [0 \ 0 \ v(t)]^T$ = noise vector in the state transition;

$X(t) = [\hat{s}_n(t) \ \hat{v}_n(t) \ \hat{a}_n(t)]^T$ = measurement vector; and

$$F = \begin{pmatrix} 1 & \Delta t & \Delta t^2/2 \\ 0 & 1 & \Delta t \\ 0 & 0 & 1 \end{pmatrix}$$



(a)



(b)

FIGURE 1 Driver behavior data measurements and Kalman smoothing results: (a) interface of Volvo ERS software and (b) comparison of measured real-time vehicle states by ERS software and off-line estimates of vehicle states by Kalman smoothing algorithm (measuring interval is $\Delta t = 0.04$ s).

As far as is known, the Kalman filter can be applied to estimate vehicle states with optimal results in the minimum mean square sense. In previous studies (15), the Kalman smoothing algorithm, also called the Rauch–Tung–Striebel smoother (16), was adopted to attain a more accurate estimate of the states of the following vehicle only based on the distance measurement—that is, $H = [1 \ 0 \ 0]$. Figure 1b shows clear speed and acceleration patterns in the car-following mode estimated from the distance measurement and the comparison with real-time estimates. Therefore, with the unique instrumented car and data estimation method, random car-following patterns can be obtained with high-accuracy estimation results comparable to those from other measurement methods. The longitudinal behavior of drivers changes under different conditions, and hence it is necessary to separate behavioral patterns of drivers in different situations (17). In a study by Bengtsson (18), four common stages were proposed: following, cut-in, braking, and approaching. Each of them adopted a unique parameter set. It was reported that the resulting model is more robust than trying to estimate a parameter set for all stages. In a previous study (19), car-following data were also classified into four regimes: approaching, stable following, braking, and accelerating. Approaching describes the process in which a vehicle starts to react to a leading vehicle and ends when the following vehicle reaches the area of the desired distance. In the stable following regime, drivers can both accelerate and decelerate mildly to keep in the area of a desired distance and this process may result in a temporary headway closing or

opening. The braking process includes more intensive deceleration behavior when the following vehicle comes too close to the leading one or the following speed is much faster than that of the leading vehicle. The acceleration process describes how the following vehicle accelerates intensively to a speed level when a leading vehicle exists. This process may result in either the closing or the opening of two cars. Figure 2 presents all car-following regimes.

SPECTRUM ANALYSIS AND DRIVER REACTION TIME ESTIMATION

In this section, spectrum analysis methods are introduced to analyze the car-following data in the frequency domain. Before the method is applied to the driver reaction delay estimation, the mathematical foundations of spectrum analysis and delay estimation methods are reviewed.

Mathematical Review

Spectrum analysis is a common methodology in system identification (20), signal processing (21), and time series analysis (22). It is based on the analysis of cross- and auto-spectrum of two stationary stochastic processes, which are defined as the Fourier transform of

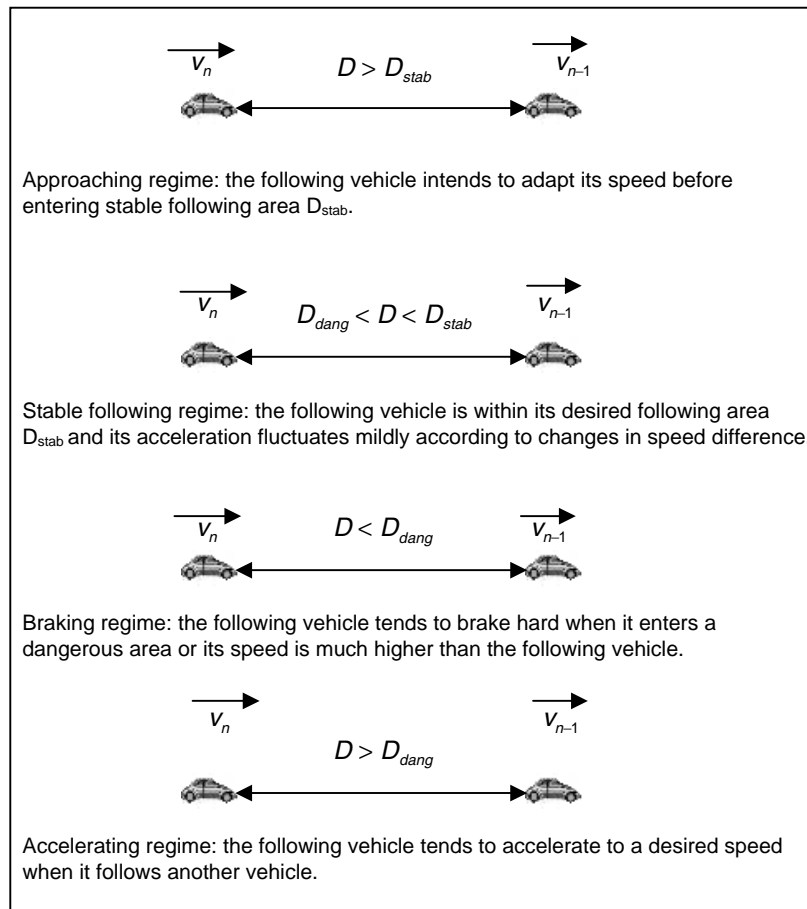


FIGURE 2 Classification of interactive car-following regimes (distance can also be represented by time).

the auto-covariance and cross-covariance functions of the process as follows:

$$C_{xy}(\omega) = \sum_{\tau=-\infty}^{\infty} \gamma_{xy}(\tau) e^{-i\omega\tau} \quad (4)$$

$$S_{xx}(\omega) = \sum_{\tau=-\infty}^{\infty} \gamma_{xx}(\tau) e^{-i\omega\tau} \quad (5)$$

where $\gamma_{xy}(\tau)$ and $\gamma_{xx}(\tau)$ are the cross-covariance function between the input $x(t)$ and the output $y(t)$ and the auto-covariance function of the input $x(t)$, respectively. The coherency spectrum is defined as the normalized cross-spectrum of $C_{xy}(\omega)$:

$$\Theta_{xy}(\omega) = \frac{|C_{xy}(\omega)|}{\sqrt{S_{xx}(\omega)S_{yy}(\omega)}} \quad (6)$$

and it is a bounded measure for the linear association between the time series. The gain spectrum is defined as

$$G_{xy}(\omega) = \frac{|C_{xy}(\omega)|}{S_{xx}(\omega)} \quad (7)$$

which describes the amplitude of the transfer function of the linear system between the input process $x(t)$ and the output process $y(t)$. The phase spectrum $G_{xy}(\omega)$ is defined by

$$\Phi_{xy}(\omega) = \arg[C_{xy}(\omega)] \quad (8)$$

or

$$C_{xy}(\omega) = |C_{xy}(\omega)| e^{i\Phi(\omega)} \quad (9)$$

The phase spectrum of a pure delay system, $H(\omega) = e^{-i\omega\tau}$, is a straight line and that is because the cross-spectrum can be written as

$$C_{xy}(\omega) = H^*(\omega)S_{xx}(\omega) \quad (10)$$

where $H^*(\omega)$ is the conjugate of the system transfer function. Moreover, because $S_{xx}(\omega)$ is real,

$$\Phi_{xy}(\omega) = \arg[H^*(\omega)] = \omega\tau \quad (11)$$

Delay Estimation Methods

There are a number of methods for estimating delay between a pair of time series or signals, which can be classified as parametric estimations and nonparametric estimations. The former is based on the mathematical modeling of time series such as ARMA models, whereas the latter tries to explore the delay by correlation and spectral analysis of data. Björklund (23) reviewed the delay estimation methods in general from a control and system identification point of view. This section focus on two nonparametric delay estimation methods using spectrum analysis.

A conventional way to estimate the delay between two time series in the frequency domain is to fit a straight line to the phase spectrum due to the relation in Equation 11. Hannan and Thomson (24) proposed fitting a straight line in the least-squares sense by finding the delay τ that maximizes the following objective function:

$$L(\tau) = \sum_{\omega_i \in B} \frac{\Theta^2(\omega_i)}{1 - \Theta^2(\omega_i)} \cos\{\arg[H(\omega_i)] - \omega_i\tau\} \quad (12)$$

where B represents available frequencies with significant coherence. The cosine function in Equation 12 is used to take care of the periodicity problem of the phase spectrum. In principle, this method gives exact delay estimation when the linear system is a pure delay system. In reality, many physical and biological systems can be modeled as a minimum phase system with an all-pass system as in Figure 3a (the Z-transform is used in the system representation), although the all-pass part may be more than a pure delay. Muller et al. (25) suggested correcting the phase by eliminating the minimum phase part, which can be estimated with the Hilbert transform method (26), and then estimating the delay by fitting a straight line to the all-pass part. The idea is to find the delay τ maximizing the updated objective function

$$L(\tau) = \sum_{\omega_i} \frac{\Theta^2(\omega_i)}{1 - \Theta^2(\omega_i)} \cos\{\arg[H(\omega_i)] - \hbar[\log|G_{xy}(\omega_i)|] - \omega_i\tau\} \quad (13)$$

where $\hbar(\log|G_{xy}(\omega_i)|)$ is the Hilbert transform of the logarithm of the gain or amplitude of the transform function of the linear system. However, this method is valid only when a broad band of coherence exists but is limited to the delay estimation between signals correlated within a narrow band (25).

Another extensively used method is based on coherence analysis, as a delay τ between time series in principle will cause a reduction in the estimated coherence between them. To compensate the reduction in coherence due to the delay, artificial shifts are applied to realign one of the time series by a lag τ while keeping the other one constant. Then the delay shift giving the maximum coherence at a significantly coherent frequency may be found. Mathematically, the idea can be represented as follows:

$$\tau_m = \arg \max_{\tau} \Theta_{xy}(\tau, \omega_0) \quad (14)$$

where ω_0 is a frequency or frequency band of significant coherence and spectral power density. This method is suitable for the delay estimation between time series of narrow-banded coherence for which the phase spectrum method cannot be reliably applied.

Validation

Both delay estimation methods of Equations 13 and 14 have been validated in a number of publications such as Muller et al. (25). To evaluate these methods scientifically before being applied to a time series, they were first validated by filtering of an input signal through a system like Figure 3a, where the all-pass part is a pure delay [i.e., $Q(Z) = 1$] and the minimum phase is set to be first- to third-order all-pole models or AR(N) models, which can be represented as follows:

$$y(t) = \sum_{n=1}^N a_n y(t) + x(t - \tau) \quad (15)$$

where $N = 1, \dots, 3$. First, the method is tested when the input is white noise. Both the phase spectrum and coherence analysis methods give a satisfying estimation of the delay time. Then the input is changed to a narrow band signal such as the measured car-following data in Figure 3b. The phase spectrum method does not lead to a satisfying result, whereas the coherence method gives a rather good estimation

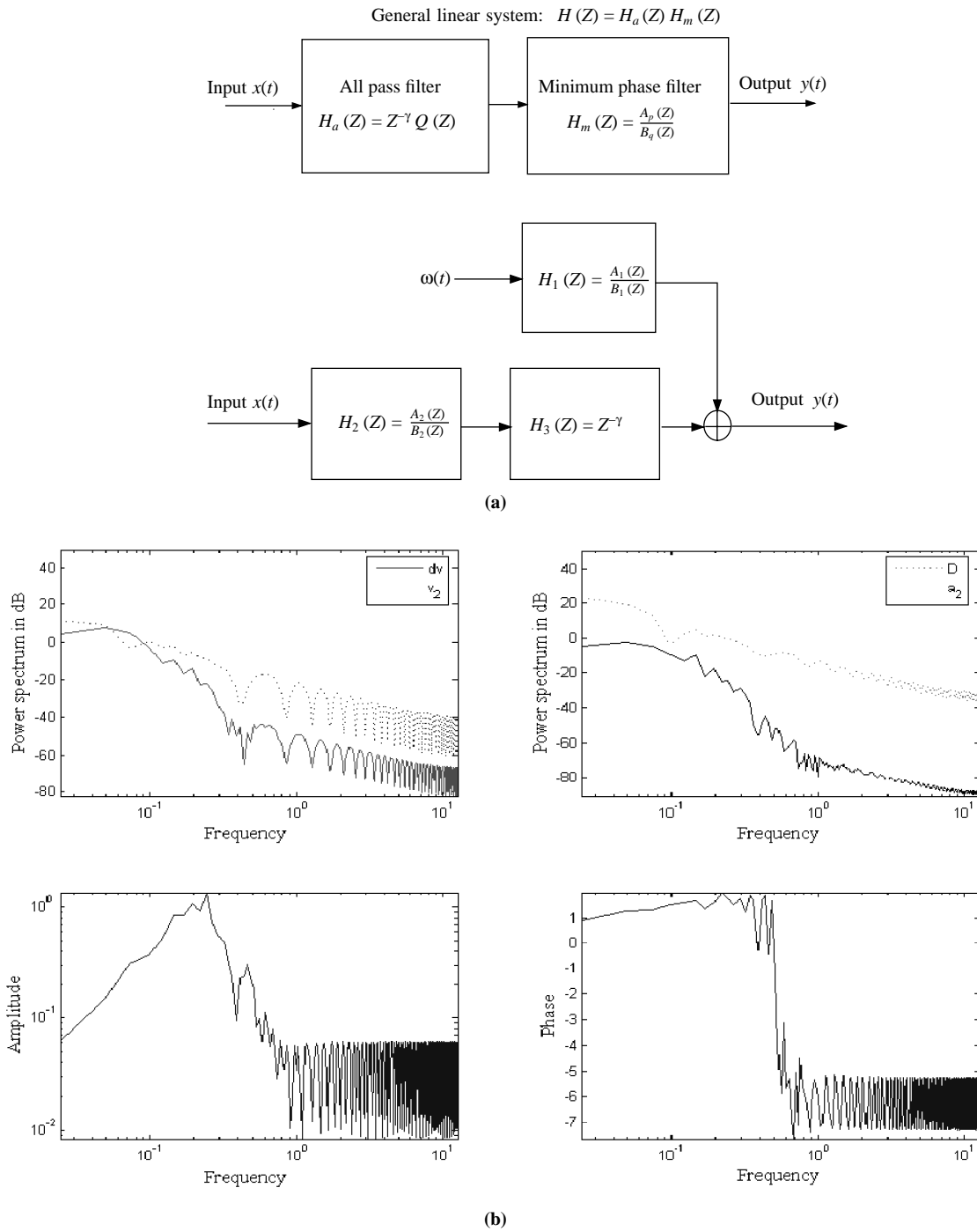


FIGURE 3 Estimation of delay within linear systems: (a) representation of general linear system by minimum phase filter and all-pass filter and validation system for delay estimation and (b) power spectrum of the time series and transfer function (amplitude and phase) between speed difference and acceleration time series.

of the delay. Further, the methods were examined by delay estimation in a more complex system in Figure 3a where $H_1(Z)$ is an ARMA(1,3) system and $H_2(Z)$ is a third-order AR system. The signal-to-noise ratio in the experiment ranges from 0 to 10 dB. When the input $x(t)$ is white noise, both methods can be successfully applied to estimate the delay (e.g., Figure 4a). When input is a narrow band signal such as the speed difference time series of the car-following data, the coherence method can be more successfully applied. It appears that coherence analysis performs better in the validation procedures for narrow band signals. However, all these tests are conducted for true linear systems, because cross-spectral analysis assumes linear and stationary properties of the input and output relation. But this assumption is always violated to some degree because of the nonlinearity and noise involvement in real-life systems. Nevertheless, the study by Barton and Cohn (27) indicates that the response of the visual system of humans to oncoming objects in a driving task exhibits a band-pass characteristic, which is well described by a linear, minimum phase, third-order transfer function. This serves as concrete support to application of the spectrum analysis methodology.

Application

After both delay estimation methods were evaluated, they were applied in the driver reaction time estimation from real car-following data. It is not easy to apply spectrum estimation because discrete Fourier transform of the finite data sequence results in the spectral leakage problem (21). In many cases, some window types W_s with smoothed edges may apply to the data to reduce the leakage when computing the periodogram, a straightforward estimator of the power spectrum. However, the periodogram is not a consistent estimator for the spectrum because its variance does not decrease when the length of data increases. In the literature, such as the work of Hayes (21), many methods have been proposed to estimate the spectrum but a trade-off always exists between the variance and the bias of the estimation. In general, the approximate variance can be derived for the gain and phase spectrum (22)

$$\text{Var}[\hat{G}_{xy}(\omega)] = \frac{1}{\nu} \left(\frac{1}{\Theta_{xy}(\omega)^2} + 3 \right) |G_{xy}(\omega)| \quad (16)$$

$$\text{Var}[\hat{\Phi}_{xy}(\omega)] = \frac{1}{\nu} \left(\frac{1}{\Theta_{xy}(\omega)^2} - 1 \right) \quad (17)$$

where ν is defined as the effective number of degrees of freedom and depends on the smoothing window W_s . Moreover, the phase estimate has its 95% confidence interval given by

$$\hat{\Phi}_{xy}(\omega) \pm 1.96 \left[\frac{1}{2M} \left(\frac{1}{\Theta_{xy}(\omega)^2} - 1 \right) \right]^{1/2} \quad (18)$$

where M is the number of disjoint segments the data sequence is divided into when the power spectra and cross-spectrum are calculated. Therefore, both the phase and the gain spectrum cannot be reliably estimated in the case of small coherency.

In the reaction delay estimation, an attempt was made to apply both methods with a variation of window types, frequency resolutions, and so forth (21). Certain criteria have been used to determine a satisfying reaction delay estimate. First, it should be within a reasonable range (e.g., 0–3 s); second, because car-following data are all narrow band signals, the delay estimated from a frequency of

narrow-banded coherence by the coherence analysis method is more reliable than the result from phase estimation in this case; finally, if the estimations from both methods are consistent or close, the result is more acceptable. Figure 4b presents an example in which there are consistent estimations of driver reaction delay using both coherence and phase analysis methods. Delays have been estimated between the speed difference inputs and acceleration outputs for 10 random drivers in the whole car-following process and the results range from 0.52 to 1.24 s. However, when both methods are applied to estimate delays between inputs of speed of the following car and distance headway and the acceleration, the methods may give inconsistent estimations and some of the estimated delays may be zero or even positive values. This might be explained by several facts. First, the linear relation between the speed of the following car (or the distance headway) and the acceleration often is not significant, and therefore the cross-spectrum method cannot be reliably applied. Second, unlike the speed difference between two vehicles, which is directly related to the changing rate of the visual range detected by the driver's eyes (27), human drivers have difficulty telling, even roughly, distance and speed values when driving. In addition, human drivers also show a certain anticipation ability, and this may give the estimated system some noncausal characteristics in their sensitivity. Consequently, it is practically more appropriate to adopt the time delay between the stimulus, the speed difference, and the acceleration reactions. Because the sample is not large enough in this study, collecting more data will be necessary to summarize the estimated reaction times as a distribution. However, the estimated results in this section can be applied for model calibration and evaluation in the next section.

EVALUATION OF GM-TYPE MODEL

In this section, a generalized GM-type car-following model is calibrated on the basis of the empirical data and the reaction time estimated by spectrum analysis. Moreover, the calibrated model is evaluated with closed-loop simulations.

Generalized GM-Type Model

First, a more generalized form of the classic GM-type model, an extension of Equation 1, is introduced, with the corresponding assumptions on this model form. At first, this generalized GM model assumes asymmetry between the acceleration and deceleration processes; moreover, it is assumed that positive speed differences will result in positive acceleration of the following car, while negative speed differences lead to deceleration of the following vehicle. Second, it is proposed that a reaction delay exists only between the speed difference stimulus and the acceleration output, whereas the sensitivity term is determined by the real-time information of space headway and following speed. Finally, it is assumed that the model parameters are different for different car-following regimes including stable following, approaching, accelerating, and braking. This means that different parameter sets are planned to be estimated for the corresponding car-following stages in the microsimulation model. Mathematically, the model is expressed by

$$\begin{aligned} \dot{a}_n^{s,g}(t + \tau_n) = & \alpha^{s,g} \frac{v_n(t + \tau_n)^{\beta^{s,g}}}{[x_{n-1}(t + \tau_n) - x_n(t + \tau_n)]^{\gamma^{s,g}}} [v_{n-1}(t) - v_n(t)] \\ & + \epsilon_n^{s,g}(t + \tau_n) \end{aligned} \quad (19)$$

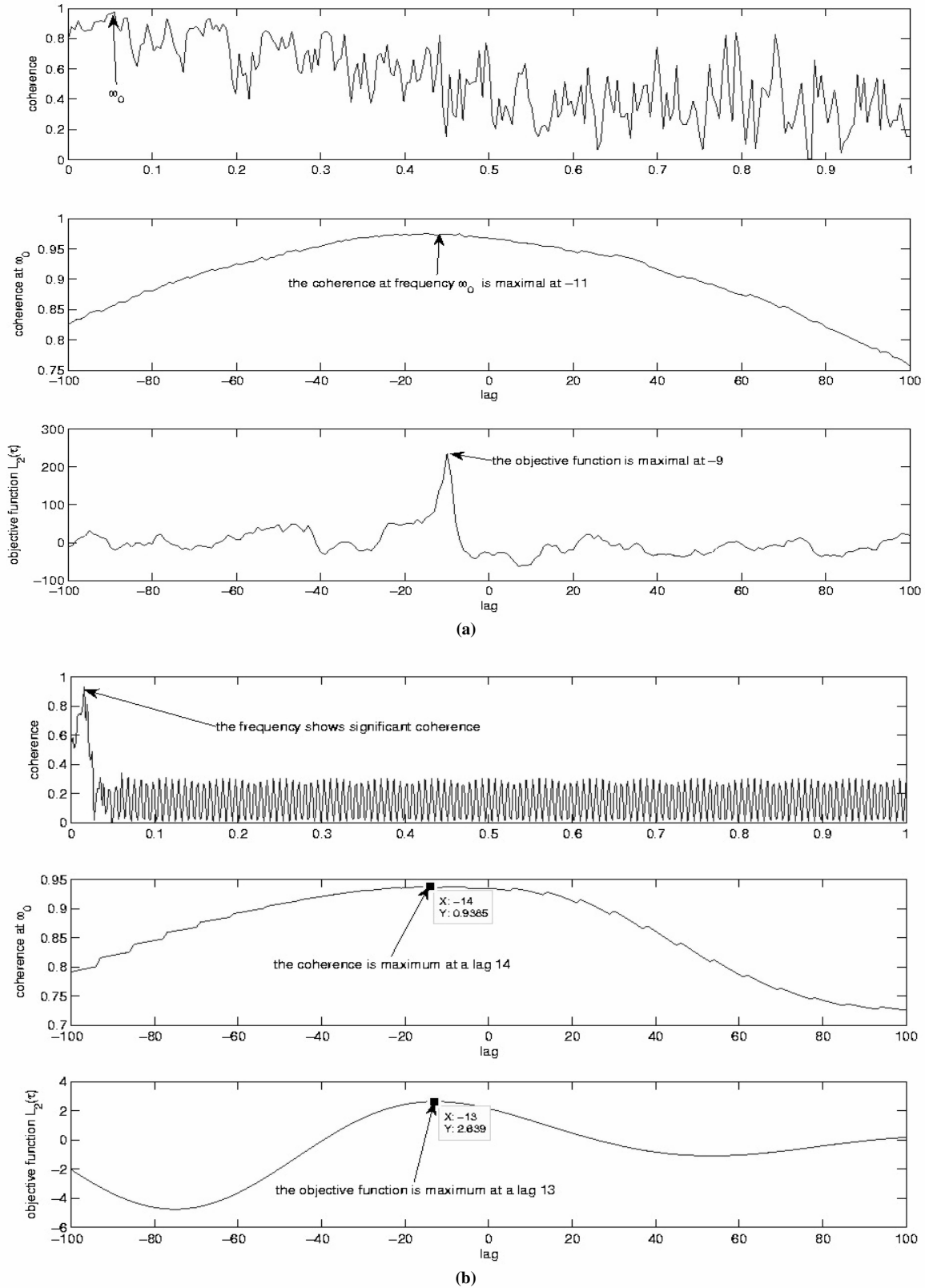


FIGURE 4 Delay estimation based on spectrum analysis: (a) validation results of delay estimation methods on the basis of pure linear system with noise (real delay is -10 and estimates from coherence and phase methods are -11 and -9, respectively) and (b) estimation of driver reaction time between speed difference and acceleration (estimated lag is -13 and interval is $\Delta t = 0.04$).

where

- $s \in \{\text{stable following, approaching, accelerating, braking}\},$
- $g \in \{\text{acceleration, deceleration}\},$
- $\tau_n = \text{reaction time to the stimulus,}$
- $\Delta v_n(t) = v_{n-1}(t) - v_n(t), \text{ and}$
- $\epsilon_n^{s,g}(t + \tau) = \text{stochastic random term at time } t + \tau_n.$

Model Calibration

The current car-following data from 10 randomly observed drivers are filtered, realigned according to the reaction delay estimation, and stored in a database using a computer program developed for this purpose. With more data collection by the instrumented vehicle, the size of the database will increase accordingly and the calibration will be repeated to include the new data sets. Results are reported mainly from calibration in the stable following regime in this article because the principle and procedure are similar for other regimes and the stable following pattern is most abundant in the data sets, but traditionally it is difficult for regression analyses. In

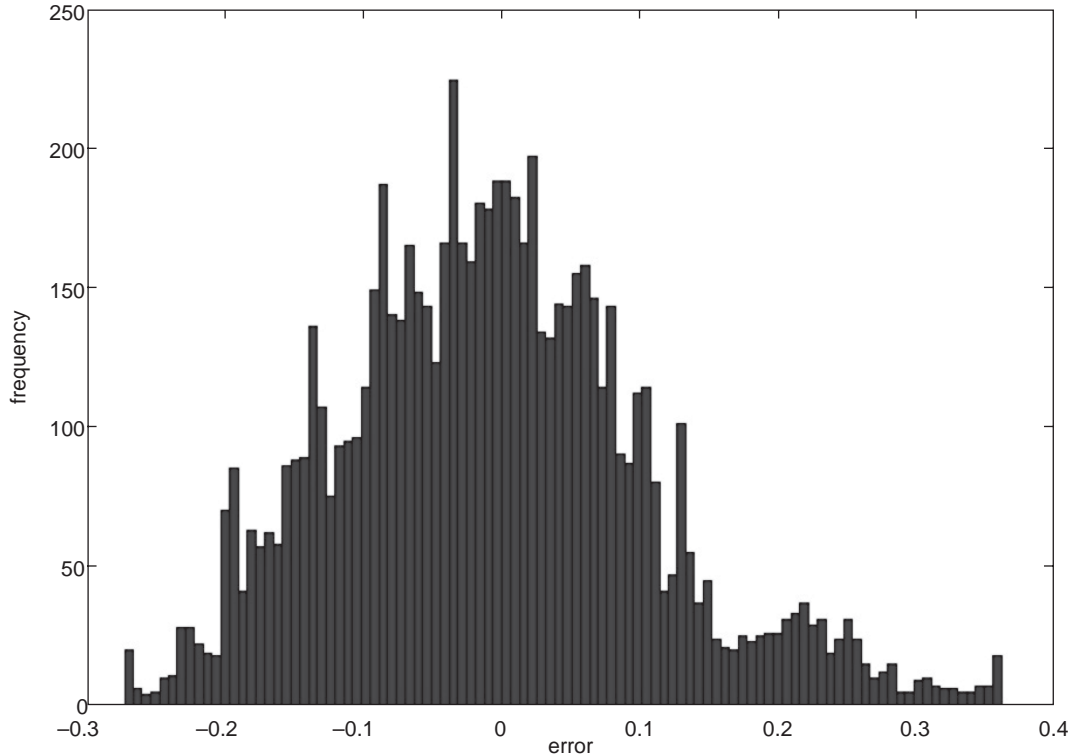
practice, the calibration is often reformulated as a nonlinear optimization problem, that is, to minimize the summation of squared errors between the model output and real output data. Mathematically, this can be represented by

$$\min_{\alpha, \beta, \gamma} \sum_i \sum_t \epsilon_n^i(t)^2 = \min_{\alpha, \beta, \gamma} \sum_i \sum_t \left\{ \tilde{a}_n^i(t) - \alpha \frac{v_n^i(t)^\beta}{[x_{n-1}^i(t) - x_n^i(t)]^\gamma} \right. \\ \left. |v_{n-1}(t - \tau_n) - v_n(t - \tau_n)| \right\}^2 \tag{20}$$

where \tilde{a}_n^i is the real acceleration of the following vehicle n for data sequence i , and the parameter sets of α , β , and γ are different for acceleration and deceleration processes. This problem can be solved numerically either by gradient-based methods (e.g., the iterative gradient search and conjugate gradient method) or by derivative-free methods (e.g., the grid search and genetic algorithm) (28). The calibration was conducted using MATLAB and Figure 5a shows the calibrated parameters for the generalized GM-type model with data

Action	Parameters		
	α	β	γ
Acceleration	0.0025	1.49	0.25
Deceleration	-5.20	1.49	2.71

(a)



(b)

FIGURE 5 Example of calibration results for generalized GM-type model in stable following regime: (a) calibrated parameters for GM-type model and (b) residual error distribution of calibration results.

from stable following regimes. Figure 5b also indicates the distribution of the stochastic residual term $\epsilon(t)$ after the calibration process.

Model Evaluation

After calibration of the model based on real data, evaluation of the model is an indispensable procedure for real applications. Because the model is calibrated on the basis of the acceleration output, it is necessary to study whether the model can replicate the speed and position profiles of the same data sequence in a closed-loop simulation in which the states of the leading car and the initial condition of the following vehicle are given and then the car-following process is simulated. Figure 6a presents an example of the comparison between the original data and simulated states using the generalized GM-type model calibrated on the same car-following data sequence. The speed profile of the following vehicle can be replicated more accurately than its positions because it is only the first-order integral of the acceleration process. The bias in certain acceleration points and therefore the speed values may result in an unredeemable error in positions of the following vehicle. Recently, Punzo and Simonelli (29) proposed formulating a dynamic calibration process as follows:

$$\min_{\theta} (\bar{x}^{\text{obs}} - \bar{x}^{\text{sim}}) C^{-1} (\bar{x}^{\text{obs}} - \bar{x}^{\text{sim}}) \quad (21)$$

where

C = covariance matrix,

θ = parameter of acceleration model [$\theta = (\alpha \beta \gamma)^T$ in the GM model],

\bar{x}^{obs} = observed measure of performances (MOPs) vector, and

\bar{x}^{sim} = MOPs vector from a closed-loop simulation based on the acceleration model and the initial condition.

This formulation generalizes the situations in which acceleration, speed, and position can be used as MOPs. It has been reported that using vehicle trajectories as MOPs gives better calibration results than using acceleration profiles. Hence, the calibration strategy can be further improved; it is also worth investigating whether the strategy will enhance the prediction ability of the model. Robustness of a model means its ability to predict the data not being used in the calibration process. In this car-following study, that can be examined by a combination of cross-validation and closed-loop simulation in which several data sequences are adopted in the calibration of the model and then a new car-following data set is validated by the outputs of a closed-loop simulation. Figure 6b presents an example of the comparison between the original data and simulated outputs using the generalized GM-type model calibrated on several other car-following data sets. From the figure, the model can basically replicate the states of the following vehicle in reality without local divergence (18), although certain bias still exists. From the cross-validations on the data sets in the stable following regime, the prediction errors are between 11% and 28% using the average gap measure (30)

$$e = \frac{\sum_{t=0}^T |s^{\text{sim}}(t) - s^{\text{obs}}(t)|}{\sum_{t=0}^T |s^{\text{obs}}(t)|} \quad (22)$$

This means that using acceleration to calibrate the model sometimes gives a high bias on the trajectory prediction of the following

car. In addition, a more justifiable criterion in the validation process might study the prediction error in the whole states of the following vehicle; that is,

$$e = \frac{\sum_{t=0}^T \sqrt{|Y^{\text{sim}}(t) - Y^{\text{obs}}(t)|^T W |Y^{\text{sim}}(t) - Y^{\text{obs}}(t)|}}{\sum_{t=0}^T \sqrt{Y^{\text{obs}}(t)^T W Y^{\text{obs}}(t)}} \quad (23)$$

where $Y(t) = [a(t) \ v(t) \ s(t)]^T$ is the state vector at time t , and W is the weight matrix.

SUMMARY AND CONCLUSION

Studying driver behavior based on data from real traffic has recently become a promising direction for understanding behavior responses of drivers, for modeling driver behavior in traffic simulation, and for designing driver assistant systems such as adaptive cruise control systems. In this paper, a car-following data collection and reduction method was presented based on an advanced-instrumented vehicle. Moreover, the coherence and phase spectrum analyses were introduced as two methods to estimate an important parameter of car-following models: the reaction time or reaction delay. The advantage of spectrum analysis is that one may directly estimate the reaction delay from the empirical data without assumptions of the model form, and the estimated value can be understood as an independent parameter of driver properties without any relation to adopted car-following models. However, the methods are limited by the linear and stationary pre-suppositions on the system and the difficulties of spectral estimations in practice. Hence, the validation of the estimated reaction times is still not sufficient and further exploration of this topic both in the time series analysis domain and in psychology aspects is still necessary. In addition, the fixed delay assumption also puts a restriction on the ability of the model to represent reality; estimating the delay as a statistical or uncertainty term on the basis of a quantitative analysis of real data may improve this deficiency. Based on the fixed reaction time estimation, a database of car following has been initiated with data sets from 10 randomly observed drivers. The classic GM-type model was modified and calibrated using data sets in the stable following regime. To test the properties of the model, closed-loop simulations were applied to evaluate the replicability and robustness of the model. The results indicate that the calibrated model can basically describe the stable car-following regime, although certain bias exists. Therefore, more effort should be devoted to exploring better strategies for dynamic calibration of the model; meanwhile, similar studies are necessary to extend to other car-following regimes and the global stability of the model should also be evaluated either analytically or in a microscopic simulation environment in future research.

ACKNOWLEDGMENTS

The authors thank Karl-Lennart Bång for his consistent support in data collection based on the advanced-instrumented vehicle. This research was undertaken as part of the SIMLAB project, which is funded by the Swedish National Road Administration (Väggerket) and the Center for Traffic Simulation Research at the Royal Institute of Technology.

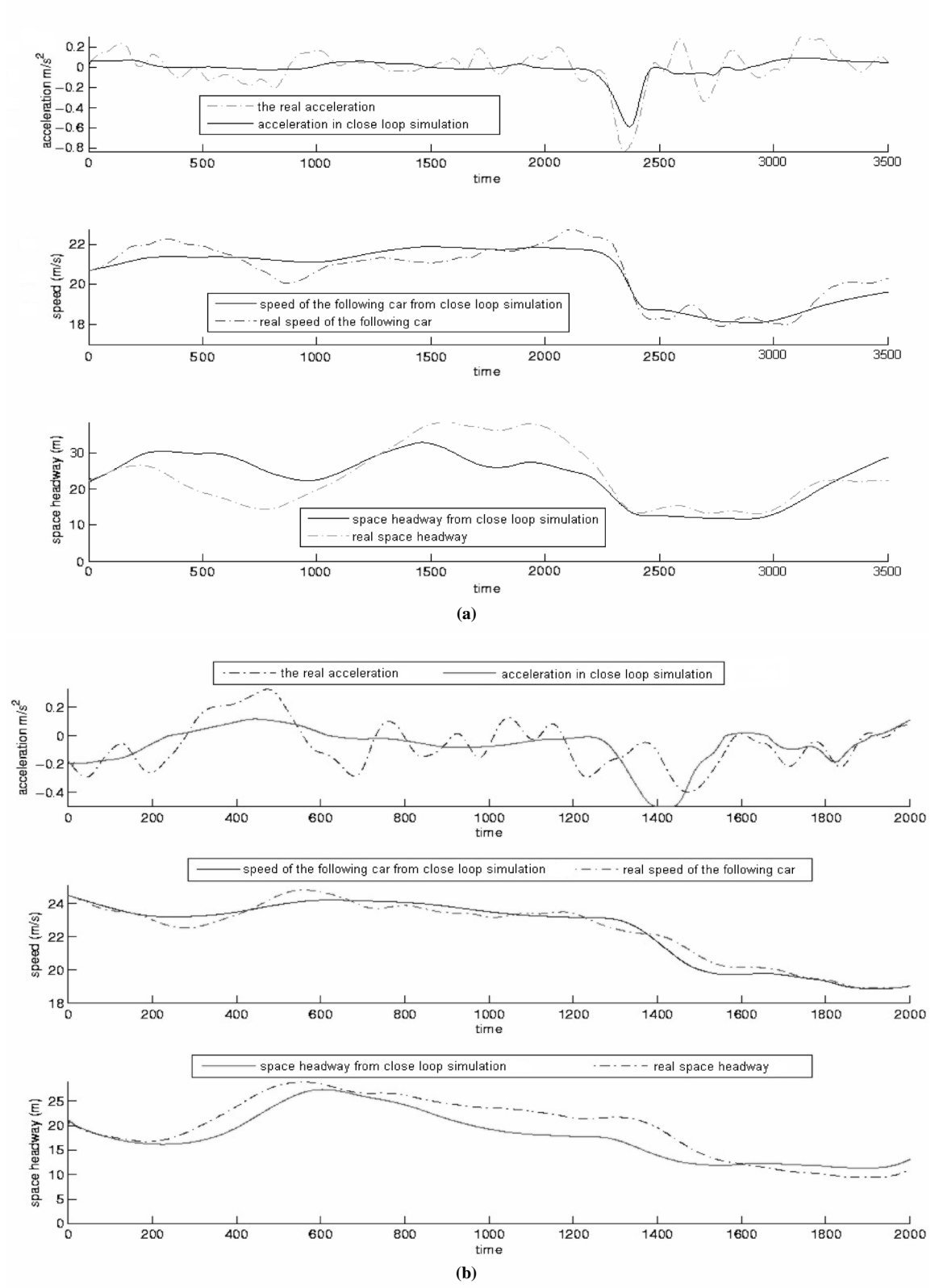


FIGURE 6 Example of evaluation results for generalized GM-type model in stable following regime: (a) comparison of real vehicle states (acceleration, speed, and position curves) with results from replication test using a closed-loop simulation and (b) comparison of real vehicle states with results from model prediction test by cross-validation.

REFERENCES

1. Gazis, D. C., R. Herman, and R. W. Rothery. Nonlinear Follow-the-Leader Models of Traffic Flow. *Operational Research*, Vol. 9, 1961.
2. Chandler, R. E., R. Herman, and E. W. Montroll. Traffic Dynamics: Studies in Car Following. *Operational Research*, Vol. 6, 1958, pp. 165–184.
3. Brackstone, M., and M. McDonald. Car Following: A Historical Review. *Transportation Research F*, Vol. 2, 1999, pp. 181–196.
4. Chakroborty, P., and S. Kikuchi. Evaluation of General Motors Based Car Following Models and a Proposed Fuzzy Inference Model. *Transportation Research C*, Vol. 7, 1999, pp. 209–235.
5. Leutzbach, W., and R. Wiedemann. Development and Applications of Traffic Simulation Models at the Karlsruhe Institut für Verkehrswesen. *Traffic Engineering and Control*, May 1986, pp. 270–278.
6. Boer, E. R., and R. V. Kenyon. Estimation of Time Varying Delay Time in Non-stationary Linear Systems: An Approach to Monitor Human Operator Adaptation in Manual Tracking Tasks. *IEEE Transactions on System, Man and Cybernetics*, 1996.
7. Gerlough, D. L., and M. J. Huber. *Special Report 165: Traffic Flow Theory: A Monograph*. TRB, National Research Council, Washington, D.C., 1975.
8. Aycin, M. F., and R. F. Benekohal. Performance of the Generalized Car-Following Model Obtained from Macroscopic Flow Relationships in Simulating Field Data. Presented at 83rd Annual Meeting of the Transportation Research Board, Washington, D.C., 2004.
9. Johansson, G., and K. Rummel. Drivers' Brake Reaction Time. *Human Factors*, Vol. 13, No. 1, 1971, p. 23.
10. T. Magister, R. Krulec, M. Batista, and L. Bogdanovič. The Driver Reaction Time Measurement Experiences. *Proceedings of Innovative Automotive Technology (IAT'05) Conference*, Bled, Slovenia, 2005.
11. Fambro, D. B., R. J. Koppa, D. L. Picha, and K. Fitzpatrick. Driver Perception-Brake Response in Stopping Sight Distance Situations. In *Transportation Research Record 1628*, TRB, National Research Council, Washington, D.C., 1998, pp. 1–7.
12. Ozaki, H. Reaction and Anticipation in the Car-Following Behavior. *Proc., 12th International Symposium on the Theory of Traffic Flow and Transportation*, Berkeley, Calif., 1993.
13. Ranjitkar, P., T. Nakatsuji, Y. Azuta, and G. S. Gurusinge. Stability Analysis Based on Instantaneous Driving Behavior Using Car-Following Data. In *Transportation Research Record: Journal of the Transportation Research Board, No. 1852*, Transportation Research Board of the National Academies, Washington, D.C., 2003, pp. 140–151.
14. Ahmed, K. I. *Modeling Drivers' Acceleration and Lane Changing Behavior*. PhD thesis. Massachusetts Institute of Technology, Cambridge, Mass., 1999.
15. Ma, X., and I. Andréasson. Dynamic Car Following Data Collection and Noise Cancellation Based on the Kalman Smoothing. *Proceedings of IEEE International Conference on Vehicular Electronics and Safety*, 2005.
16. Hakin, S. *Kalman Filtering and Neural Networks*. John Wiley and Sons, New York, 2001.
17. Kim, T., D. J. Lovell, and Y. Park. Limitations of Previous Models on Car-Following Behavior and Research Needs. Presented at 82nd Annual Meeting of the Transportation Research Board, Washington, D.C., 2003.
18. Bengtsson, J. *Adaptive Cruise Control and Driver Modeling*. PhD thesis. Lund Institute of Technology, Sweden, 2001.
19. Ma, X., and I. Andréasson. Behavior Measurement, Analysis and Regime Classification in Car-Following. *IEEE Transactions on Intelligent Transportation Systems*, 2006, in press.
20. Johansson, R. *System Modeling and Identification*. Prentice Hall, Englewood Cliffs, N.J., 1993.
21. Hayes, M. H. *Statistical Digital Signal Processing and Modeling*. John Wiley and Sons, Toronto, Ontario, Canada, 1996.
22. Brockwell, P. J., and R. A. Davis. *Time Series: Theory and Methods*. Springer, New York, 1991.
23. Björklund, S. *A Survey and Comparison of Time-Delay Estimation Methods in Linear Systems*. PhD thesis. Linköping University, Sweden, 2003.
24. Hannan, E. J., and P. J. Thomson. Delay Estimation and Estimation of Coherence and Phase. *IEEE Transaction: Acoustics, Speech, Signal Process*, Vol. 29, 1981, pp. 485–490.
25. Muller, T., M. Lauk, M. Reinhard, C. H. Luking, and J. Timmer. Estimation of Delay Times in Biological Systems. *Annals of Biomedical Engineering*, Vol. 3, 2003, pp. 1423–1438.
26. Oppenheim, A. V., and R. W. Schaffer. *Digital Signal Processing*. Prentice Hall, Englewood Cliffs, N.J., 1975.
27. Barton, J. E., and T. E. Cohn. Dynamic Estimation of Oncoming-Vehicle Range and Range Rate: Assessment of Human Visual System's Capabilities and Performance. Presented at 84th Annual Meeting of the Transportation Research Board, Washington, D.C., 2005.
28. Jang, J.-S., C.-T. Sun, and E. Mizutani. *Neuro-Fuzzy and Soft Computing: A Computational Approach to Learning and Machine Intelligence*. Prentice Hall, Englewood Cliffs, N.J., 1997.
29. Punzo, V., and F. Simonelli. Analysis and Comparison of Microscopic Traffic Flow Models with Real Traffic Microscopic Data. In *Transportation Research Record: Journal of the Transportation Research Board, No. 1934*, Transportation Research Board of the National Academies, Washington, D.C., 2005, pp. 53–63.
30. Brockfeld, E., R. D. Kühne, and P. Wagner. Calibration and Validation of Microscopic Traffic Flow Models. In *Transportation Research Record: Journal of the Transportation Research Board, No. 1876*, Transportation Research Board of the National Academies, Washington, D.C., 2004, pp. 62–70.

The Traffic Flow Theory and Characteristics Committee sponsored publication of this paper.